Bulletin of the Seismological Society of America, Vol. 96, No. 2, pp. 519–535, April 2006, doi: 10.1785/0120050090

Long-Period Effects of the Denali Earthquake on Water Bodies in the Puget Lowland: Observations and Modeling

by A. Barberopoulou, A. Qamar, T. L. Pratt, and W. P. Steele

Abstract Analysis of strong-motion instrument recordings in Seattle, Washington, resulting from the 2002 M_w 7.9 Denali, Alaska, earthquake reveals that amplification in the 0.2- to 1.0-Hz frequency band is largely governed by the shallow sediments both inside and outside the sedimentary basins beneath the Puget Lowland. Sites above the deep sedimentary strata show additional seismic-wave amplification in the 0.04- to 0.2-Hz frequency range. Surface waves generated by the M_w 7.9 Denali, Alaska, earthquake of 3 November 2002 produced pronounced water waves across Washington state. The largest water waves coincided with the area of largest seismic-wave amplification underlain by the Seattle basin. In the current work, we present reports that show Lakes Union and Washington, both located on the Seattle basin, are susceptible to large water waves generated by large local earthquakes and teleseisms. A simple model of a water body is adopted to explain the generation of waves in water basins. This model provides reasonable estimates for the water-wave amplitudes in swimming pools during the Denali earthquake but appears to underestimate the waves observed in Lake Union.

Introduction

Seismic waves produced by the M_w 7.9 Denali, Alaska, earthquake of 3 November 2002, initiated a series of water waves that damaged at least 20 houseboats along the shores of Lake Union and Portage Bay in Seattle, Washington, at an epicentral distance of 2400 km (Table 1; Barberopoulou *et al.*, 2004). Observers reported a series of waves, or runup of water on the shore on a calm day, at the approximate arrival time of the surface waves from the Denali earthquake. The houseboats are routinely subjected to waves from large ships and windstorms, so the damage during the earthquake suggests water waves with unusual amplitudes or periods. In Table 2 we summarize water-wave observations in Washington state during several large distant and local earthquakes to show that seiching is a recurrent phenomenon in Washington.

Seiche is a common term used to describe the standing oscillations setup in a lake or harbor due to a perturbation of the water level (Russell and Macmillan, 1952). Seismically induced seiches fall into two categories: (1) free seiches initiated by displacement of water due to fault motion or landslides (Russell and Macmillan, 1952; Ichinose *et al.*, 2000); and (2) forced seiches caused by the passing of seismic waves. The latter category, which we focus on in this article, can initiate oscillations either through the tilting of the water body or from the horizontal motion of the sides (Kvale, 1953; Russell and Macmillan, 1952; Donn, 1964; McGarr, 1965; McGarr and Vorhis, 1968; Barberopoulou *et al.*, 2004; Cassidy and Rogers, 2005). McGarr (1965) argues that for small bodies of water the angle of tilt is so slight that horizontal motions of the sides of the water body are a much more effective wave generator.

The unusual water waves observed in the Puget Lowland of Washington state following the Denali earthquake were apparently initiated by large seismic surface waves directed preferentially along the west coast of North America by the earthquake source mechanism (Eberhart-Phillips *et al.*, 2003; Barberopoulou *et al.*, 2004; Cassidy and Rogers, 2005). The concentration of water wave reports above the Seattle sedimentary basin (Barberopoulou *et al.*, 2004), suggests that local amplification of seismic waves by the basin may have played a role.

Unusual water waves in Washington state have coincided temporally with seismic-wave arrivals from past regional and distant earthquakes. Unlike previous earthquakes known for generating seiches (e.g., the 1964 Alaska earthquake), the Denali earthquake was well recorded on a variety of seismometers worldwide and has provided an opportunity to examine ground motions that initiate seiches in water bodies at large distances. Although documented damage from seiches during past seismic events has been minor in Washington state the question remains whether amplified long-period waves by sedimentary basins could cause high-amplitude water waves during large earthquakes on local crustal faults or on the Cascadia subduction zone. Examples

Table 1
Reports of Unusual Water Activity in Washington* on 3 November 2002

	Location	Duration of Water Activity in Seconds (Unless Otherwise Noted)	Period of Oscillation in Seconds (Unless Otherwise Noted)	Damage Reported	Horizontal Motion or Runup	Amplitude of Vertical Oscillation	Other Comments/Observations
1	Portland, OR					Several inches	Floating walkway was moving up and down by several inches.
2	Seattle, WA		18–23			2–3ft	Water at the Volunteer park reservoir oscillated 20–30 ft crest to crest about 8–10 times in 3 min. Observer appears to have noticed 2 different types of water motion.
3	Lake Wenatchee State Park, WA				5 ft		Lake shoreline water surged 5 ft up the beach.
4	Seattle, WA†				8–10 ft		Barge in a shipyard along with other vessels ranging from 1000 to 5000 tons experienced a violent sway.
5	Bellingham, WA	1 min	5				Reporter specified rocking of boat was in the north–south direction.
6	Seattle, WA†			Houseboat sewer, phone, and power lines were broken.			Five houseboats disconnected from dock. Dock moved few inches.
7	Seattle, WA†	1 min		Houseboat slammed against pllings, lost phone, sewer, and power lines. Mooring attachments damaged or thrown out of alignment.			Similar damage was noticed by one resident during the 1964 Alaska earthquake but not during the Nisqually event.
8	Blaine, WA	Several minutes				1 ft	Swimming pool sloshed back and forth.
9	Bellevue, WA						Swimming pool sloshed over its sides.
10	Bothell, WA	20					Water moved up and down and canoe fell off the dock into the water.
11	Silver Creek, WA					11–12 inches	Extreme water motion not accompanied by felt ground motion. Violent shaking of the lake was compared with stirring like shaking a jug of water. Lake was calm before and after the event.
12	Bayview, ID	15 min			20 inches		Docks moving laterally.
13	Seattle, WA	Few min					Swimming pool closed for the winter splashed.
14	Seattle, WA†	30					Rocking of boat.
15	Woodinville, WA						Water splashed out of the pool in the north–south direction.
16	Kirkland, WA						Sloshing observed in swimming pool.
17	Bellevue, WA						Water sloshed over the swimming pool.
18	Seattle, WA	2–5 min				1 ft	Seattle University Center: two pools showed unusually large water waves. Swimmers experienced dizziness and symptoms like sea sickness. People in other parts of the building experienced nothing.
19	Everett, WA						Sloshing observed in swimming pool.
20	Seattle, WA					10 inches	Sloshing observed along the length of the pool in city of Seattle pool.
21	Seattle, WA†			Houseboats slammed against dock pilings with water and sewer lines damaged.			Bystanders commented on this different wave action compared with that from a passing ship or caused by winds.
22	Everett, WA	30					Extreme shaking of boats back and forth.
23	Seattle, WA†	45					Houseboats unfastened from their docks (heavy appliances fell out).
24	Stanwood, WA						Water motion in Lake Martha was compared with tidal. Some swirling also observed.

(*continued*)

Table 1
Continued

25	Bainbridge Island, WA						Water moved back and forth and flowed out of the swimming pool.
26	Forest Grove, OR				3–4 ft		Henry Haag Lake had water waves of 3–4 ft moving across lake.
27	Clyde Hill, WA						Pond flooded, with 2 ft waves present.
28	Bellevue, WA†			Boats moored at marina were violently moved against the dock structures (minor damage at the docks).			Boat moving violently. Could not stand still on it without support.
29	Bellevue, WA						Water at swimming pool sloshing back and forth on a very sunny calm day without any wind.
30	Snoqualmie, WA	1 min					Thin layer of ice covering Melakwa Lake broke drawing the attention of hikers from the cracking sounds. Water rose and fell.
31	Seattle, WA	3 min				6 inches	Pool on the 35th floor of a steel/concrete building started sloshing back and forth in the north–south direction.
32	Bainbridge Island, WA						Sloshing observed on the swimming pool which overflowed.
33	Seattle, WA	180	15		4–5 ft		Docks moved violently in a north–south direction with a lot of noise.
34	Seattle, WA	60					Boat in marina moved.
35	Snoqualmie Pass, WA						Observer noticed water moving back and forth carrying ice that had broken from the icy surface.
36	Seattle, WA	30–60			3 ft		Boat started moving sideways. No vertical displacement noticed.
37	Seattle, WA†						Observer on a boat in Lake Union, moved while observing many other boats moving back and forth.
38	Seattle, WA	5 min					Water sloshed back and forth resulting in swimming pool overflowing.
39	Seattle, WA†					4–5 inches	Observer noticed water runup on the shore as the level of the water rose and fell (kayak with observer moved east–west). 4–5 cycles of complete oscillation were noticed.
40	Des Moines, WA	2–8 min					Water in fish bowl started swaying along with other things in the room, like hanging plants.
41	Des Moines, WA		<30	Boat slammed against dock.			No wind, water quiet when suddenly the boat slammed against the dock.
42	Seattle, WA	15+		Boats bumping against docks.			Boats moving back and forth. No wind was present. Shaking was quite violent.
43	Everett, WA	15					Boats in the shed moved sideways.
44	Everett, WA	60					Sloshing observed on swimming pool.
45	Mt. Rainier National Park, WA	Several minutes		Small logs washed on the shore.		3 ft	On Blue Lake near Mt. Baker, motion of the water was compared to water in a bathtub (on southwest–northeast direction).
46	Clinton, WA	30			4 ft		Observer on top of a boat noticed a sudden movement of boat and what appears to be 4 ft of runup on shore.
47	Lopez Island, WA					3 inches	Concentric wave pattern on Mud Bay, Lopez Island.
48	Marysvllle, WA	5 min					Dock swayed sideways (east–west); a boat stretched its mooring lines.
49	University Place, WA	5					Movement in pond observed.
50	Centralla, WA						Reservoirs of capacity of 3.5 and 4 million gallons oscillated.
51	Ione, WA					1 ft	Waves on Long Lake near Spokane.
52	Kenmore, WA	5 min at least					Door swang closed, river water sloshing in the north–south direction, big boat banging.

*Few other locations outside of Washington are also listed.
†Locations in Lake Union or Portage Bay.
‡Locations in Lake Washington.

Table 2
Reports of Unusual Water Waves in Seattle during other Earthquakes

Event	Observations
29 November 1891 Port Townsend earthquake	Lake Washington, on the east side of town, was lashed into foam and the water rolled onto the beach two feet above the mark of the highest water and eight feet above the present stage (*The Oregonian*, 29 November 1891; Holden, E. S (1898). A Catalog of Earthquakes on the Pacific Coast 1769–1897, Smithsonian Miscellaneous Collections, 1087).
Yakutat Bay 1899 Alaska earthquake	A 6–10 foot upheaval was observed in the center of Lake Chelan. Waves rolled toward the shore but no wind was blowing at the time (Dow, 1964).
18 April 1906 (San Francisco, California, earthquake)	"Lake Washington Feels The Shock" Surface of water on west side violently agitated. • Floats tossed about. • Three distinct tidal waves reported to have come from northeast. Seattle got a seismic disturbance, too, though it was quite short and luckily did hardly a dollar's worth of damage. About 6 o'clock yesterday morning Lake Washington on the west shore was agitated so violently that house boats, floats and bathhouses were jammed and tossed about like leaves on the water. Beyond breaking a few moorings and causing a small-sized fright, no damage (*Seattle Post-Intelligencer*, 19 April 1906). A man, who was on the bank of the Wishkah River early in the morning, said that waves five feet high rolled up the river from the sea, and that he was sure that there was some disturbance (*Seattle Post-Intelligencer*, 25 April 1906).
M 7.1 13 April 1949 Olympia earthquake	A crew towing two gravel barges reported the disturbance from their boat (*The Seattle Times*, 14 April 1949). A diver in the Seattle Port of Embarkation, working on the propeller shaft of an Army transport reported the ship "jumping." Water tanks in Snohomish overflowed.
M 9.2 27 March 1964 Good Friday Alaska earthquake	Effects felt in many states, including Washington (McGarr and Vorhis, 1968) where many houseboats were damaged.
M 6.5 28 April 1965 Seattle-Tacoma earthquake	Green Lake in North Seattle was "sloshing back and forth like soup in a shallow bowl" (*The Seattle Times*, 30 April 1965).

of such damage to docks and ships, coastal inundation, erosion of coastal areas, damage to floating bridges, or triggering of landslides on eroding bluffs has occurred in past earthquakes in other areas (e.g., Korgen, 1995; Ruscher, 1999). The 1959 *M* 7.1 Hebgen Lake, Montana, earthquake was responsible for damage to the Hebgen dam when a seiche caused water to overtop the dam several times. The 2003, *M* 8.3 Tokachi-oki earthquake in Japan caused sloshing in oil and naphtha tanks, resulting in sparks that started a fire that burned for several days (Koketsu *et al.*, 2005).

Seismic waves from the Denali earthquake recorded on the Pacific Northwest Seismic Network (PNSN; Fig. 1) show substantially larger amplitudes and longer durations within the Seattle basin (Fig. 2) (Barberopoulou *et al.*, 2004) than at surrounding sites. We use spectral ratios of these recordings (Fig. 2) to examine the amplification of the shear and surface waves from the Denali earthquake caused by the Seattle basin and the shallow glacial deposits inside and outside the basin. To estimate the influence of these amplified seismic waves on the overlying water bodies we model the generation of water waves by the amplified ground motions from the Denali earthquake using a simple 1D model (Lamb, 1932; Russell and Macmillan, 1952; Proudman, 1953; McGarr, 1965; Wilson, 1972). Although simple, the model successfully reproduces the character of waves observed in swimming pools during the Denali event but probably underestimates the observed water motions in Seattle-area natural waterways. We also discuss the apparent absence of seiche reports during the Nisqually earthquake. We use the 2001 M_W 6.8 Nisqually earthquake ground motions to drive the model because the Nisqually-type events are the region's most common type of damaging earthquakes.

Puget Lowland Geology

The Puget Lowland of Washington state is part of the Puget-Willamette forearc basin above the subducting Juan de Fuca oceanic plate (Crosson and Owens, 1987; Galster and Laprade; 1991). The Seattle basin is one of three large sedimentary basins beneath the Puget Lowland, the others being the Everett and Tacoma basins (Fig. 1) (Johnson *et al.*, 1994, 1996; Pratt *et al.*, 1997; Brocher *et al.*, 2001). The Seattle basin is a 30 km by 60 km depression in the Eocene volcanic basement rocks, filled with up to 9 km of low-density, low-velocity sedimentary rocks and unconsolidated sediments (Johnson *et al.*, 1994; Pratt *et al.*, 1997; ten Brink *et al.*, 2000; Brocher *et. al.*, 2001). The south end of the Seattle basin is formed by the Seattle Fault zone, an east-trending reverse or thrust fault separating thick sediments to the north from shallow bedrock and thin sediments to the south (Johnson *et al.*, 1994; Pratt *et al.*, 1997; ten Brink *et al.*, 2000, Brocher *et al.*, 2004). The Seattle Basin is bounded on the west by the Olympic Mountains, but its eastern boundary is not well constrained. To the north the basin sediments thin onto the antiformal Kingston Arch (Johnson *et al.*, 1994; Pratt *et al.*, 1997; ten Brink *et al.*, 2000). The

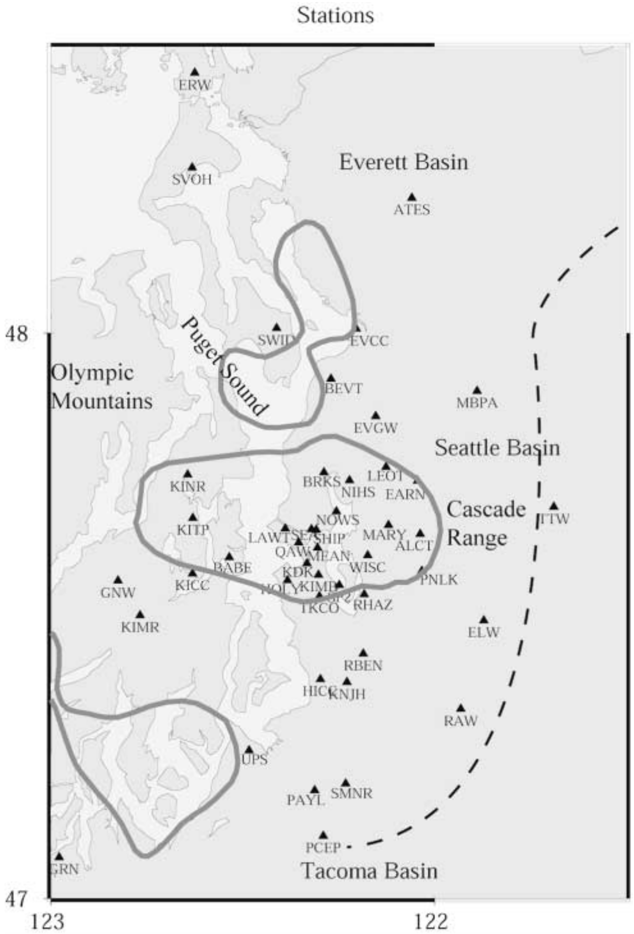

Figure 1. Map showing the strong-motion stations of the Pacific Northwest Seismic Network (PNSN) that were operating during the Denali earthquake. Stations GNW and ERW (top and left of figure) are the bedrock sites we used as reference stations for the spectral ratios. Contours show the outlines of the deep sedimentary basins and the dash-dotted contour the approximate edges of the Quaternary glacial deposits that underlie the Puget Lowland (Booth, 1994).

Everett and Tacoma basins to the north and south are less well known but also appear to be fault-bounded basins of comparable size and age to the Seattle basin (Van Wagoner *et al.*, 2002; Johnson *et al.*, 1996, 2004; Snelson *et al.*, 2000; C. M. Snelson *et al.*, unpublished manuscript, 2006).

The upper portions of the sedimentary basins are Quaternary glacial deposits that also extend across the Puget Lowland outside of the basins (Fig. 1) (Booth, 1994; Jones, 1996). These glacial deposits were laid down during a series of Quaternary ice-sheet advances and retreats, the most recent retreat being 14,000 to 12,000 years ago (Thorson, 1980). The glacial strata consist of advance deposits that were compacted when overridden by the ice and uncompacted recessional deposits that have never been covered by glaciers. The deep valleys (Puget Sound, Lake Washington) were carved by subglacial meltwater (Booth, 1994).

Sedimentary basins in the Puget Lowland are documented to amplify seismic waves at periods of 0.14 to 10 sec (Frankel and Stephenson, 2000; Frankel *et al.*, 2002; Pratt *et al.*, 2003; Pratt and Brocher, 2006). Impedance contrasts and resonance within the basin sediments explain, in part, the observed amplification, but locally generated basin surface waves likely play an important role in the long durations of ground motion. Pratt *et al.* (2003) measured the amplification across the Seattle basin relative to bedrock sites in the Olympic mountains, concluding that the maximum spectral amplification is about 16 at a frequency of about 0.33 Hz (3-sec period). They could not separate the effects of the deep basin from those of the shallow deposits because of their limited distribution of seismographs.

It has been suggested that basin subsidence results in the concentration of water bodies over the sedimentary basins of the Puget Lowland (Fig. 1) (Pratt *et al.*, 1997). The Tacoma basin underlies the many broad arms of southern Puget Sound. The Seattle basin underlies sections of Hood Canal, Puget Sound, Lake Washington, and Lake Sammamish. The Everett basin underlies Puget Sound where it widens near the Strait of Juan de Fuca. This concentration of water bodies over basins that amplify long-period seismic waves could explain the many observations of water waves during large earthquakes as noted by McGarr and Vorhis (1968).

Amplification of Seismic Waves from the Denali, Alaska, Earthquake by the Deep Seattle Basin Strata and Shallow Glacial Deposits

Data

To measure the effects of local geology on the amplitudes of the seismic waves, we calculated spectral ratios (SR) of the Denali shear and surface waves recorded at nonbedrock sites, relative to shear and surface waves recorded at bedrock sites ERW and GNW. Data consisted of three-component recordings from 46 PNSN strong-motion stations distributed around the Puget Lowland, both inside and outside the Seattle sedimentary basin (Fig. 1). The data analyzed in this article were recorded by force-balance accelerometers with flat response to acceleration for the frequency range 0–50 Hz (K2 and Guralp instruments). PNSN broadband stations also recorded arrivals from the Denali earthquake, but nearly all these instruments (many colocated with a strong-motion instrument) clipped during the surface-wave arrivals and were therefore not useful. The strong-motion instrument recordings showed an emergent but clear *S*-wave arrival, but dispersed surface waves were by far the largest waves (Fig. 2). Basin sites consistently had the greatest amplitudes and longest duration (300 sec; Fig. 2). Large-amplitude surface waves radiating to the southeast from the epicenter resulted in long-period effects across a wide region of Canada and the United States, similar to those from the 1964 Good Friday, Alaska, earthquake (Cassidy and Rogers, 2005; Eberhart-Phillips *et al.*, 2003; Barberopoulou *et al.*,

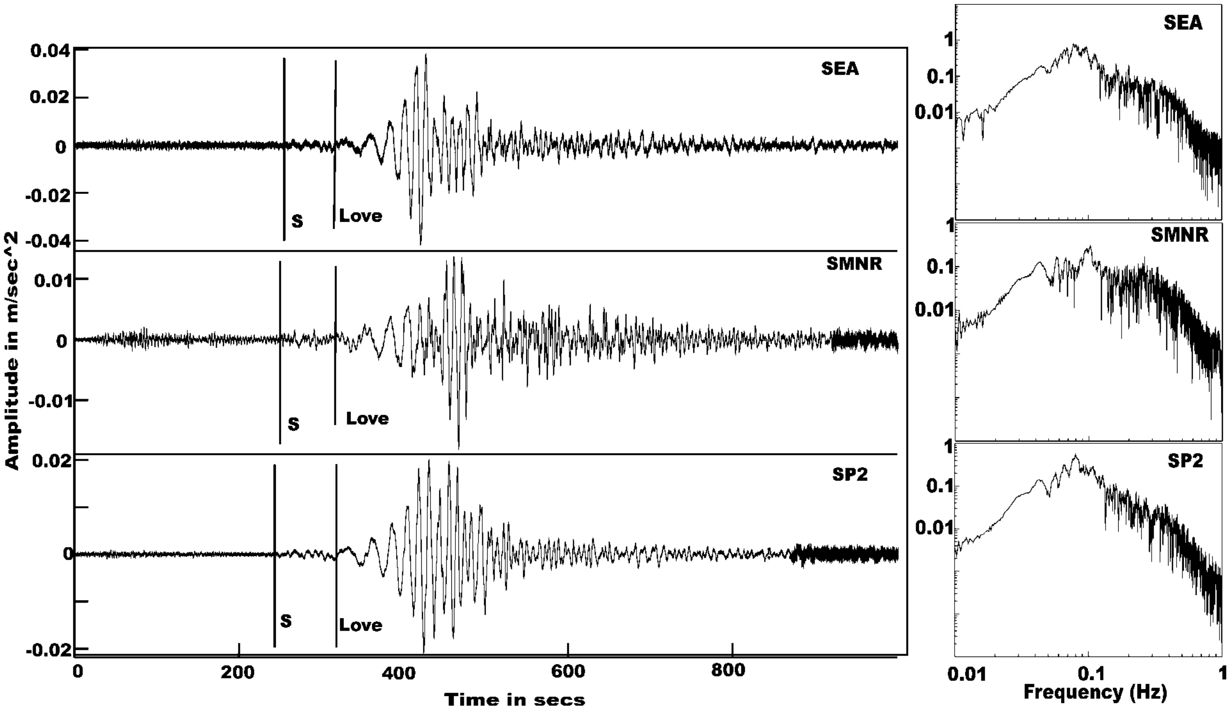

Figure 2. Seismograms from bedrock and basin sites, with traces scaled to equalize their maximum values (acceleration units are m/sec^2). The traces show the east–west component of motion recorded at stations SEA (Seattle basin), SMNR (nonbasin) and SP2 (Seattle basin). Note the extremely large surface-wave amplitudes. The maximum acceleration was about 5 cm/sec^2, and the maximum displacement was about 20 cm (40 cm peak-to-peak). On the right are acceleration spectra of these traces showing the dominant frequency in the signal to be at about 0.08 to 0.1 Hz (10- to 12.5-sec periods).

2004). Maximum acceleration on strong-motion records was 5 cm/sec^2 (0.004g) at basin sites and 1.5 cm/sec^2 at bedrock sites.

The recorded waves provide a frequency spectrum for analysis of 0.01–0.5 Hz (2- to 100-sec period), with the largest amplitudes being at frequencies of 0.08–0.1 Hz (10 to 12.5-sec periods; Fig. 2). To avoid results that are unduly influenced by a single reference station, our spectral ratios are computed relative to the average of the spectra from two bedrock sites. Reference site GNW is located on Green Mountain near Bremerton on intrusive bedrock (Eocene mafic igneous rock) and ERW is on Fidalgo Island near Anacortes on volcanic basement rock (Mesozoic intrusive rocks and associated metamorphosed strata). Relative to a time window before the P-wave arrivals, the signal-to-noise ratio for both shear and surface waves at the two bedrock reference sites (ERW and GNW), which show some of the lowest signal strengths, is greater than 2 at frequencies between 0.01 and 0.3 Hz (3.33- to 100-sec periods; Fig. 3). The signal-to-noise ratio at other sites, which generally have larger amplitudes than the reference sites, exceeds 2 up to frequencies of about 0.8 Hz (1.25 sec periods; Fig. 3). Thus, the spectral ratios we derive are reliable between 0.01 and 0.3 Hz (3.33- to 100-sec periods). Between 0.3 and 0.8 Hz,

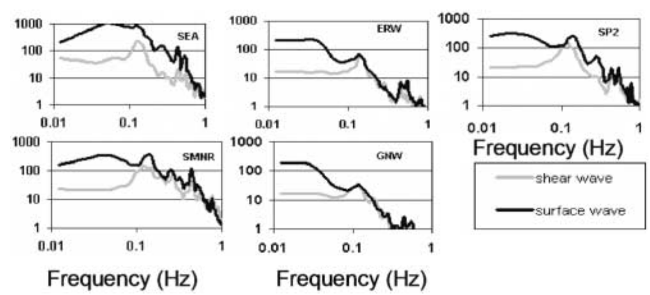

Figure 3. Plots of signal-to-noise ratio for shear and surface waves shown in Figure 2 and reference sites ERW and GNW. The signal-to-noise ratio is above 2 for the frequency range of 0.01–0.8 Hz at most of the sites except at rock sites, where the signal-to-noise ratio approaches 2 at about 0.3 Hz. Thus, spectral ratios taken with respect to the average of the two rock sites are reliable to frequencies up to 0.3 Hz. Between 0.3 and 0.8 Hz the spectral ratios are contaminated by noise in the rock signals, indicating that the computed amplifications will be underestimated because noise will make the rock reference signals artificially large.

noise at the reference sites likely will cause the spectral ratios to underestimate the amplification factors.

Processing

The spectral ratios we computed include the effects of the source parameters, wave path, station location, and instrument response (e.g., Hartzell, 1992). For teleseisms, the source and path effects can be considered the same for nearby sites because the differences in radiation angle and path are minor (azimuthal angles for the Denali earthquake ranged between east-southeast (127°) and east–southeast (130°) degrees). The SR technique assumes that the hard-rock site does not materially affect the amplitude spectrum of the waves, and the frequency spectra at the rock sites are therefore characteristic of the input source spectrum. Under these assumptions, the SR technique gives the amplification factor at the site of interest.

We chose a 70-sec time window to compute the spectra of the shear-wave arrivals, with the window length being limited by the arrival of the surface waves. A 300-sec window starting at the Love wave arrivals was used for surface-wave analysis; this time window covered the largest-amplitude arrivals (Fig. 2). Data were tapered with a 5% Hanning taper before computing the spectra. Both horizontal components of the seismograms (vector sum of the spectra) were used in the calculation of the spectral ratios. The spectral ratios were smoothed with a three-point mean smoothing algorithm. Because we have recordings from stations on both deep-basin (20 sites) and shallow glacial deposits (15 sites), we have the opportunity, unlike previous studies, to characterize the seismic-wave amplification in these two settings. We divided the sites into three categories to differentiate the amplification effects caused by the shallow and deep sediments: (1) sites over the basins (more than 2 km of strata), (2) sites on glacial deposits and older sediments outside of the deep basin (less than 2 km of sedimentary strata), and (3) sites where bedrock is very near the surface (estimated to be <20 m based on proximity to bedrock outcrops). We classified our sites as "deep-basin" if they lie over the deep portions of the basins defined by the contours in Figure 1. All our deep-basin seismograph sites lie on the Seattle basin. Seismographs at non-basin sedimentary sites lie on glacial deposits and Tertiary sedimentary rocks outside of our deep-basin contours, meaning the total thickness of sediment with a *P*-wave velocity less than 3.5 km/sec is about 2 km or less based on tomography and gravity measurements (Van Wagoner *et al.* 2002). We used the 3.5 km/sec contour as representing strong, consolidated sedimentary rocks lying near crystalline basement. Bedrock sites are known to lie on only a thin (<20 m) cover of till or sediment above metamorphic or volcanic rock.

Results

The most obvious result evident from our spectral ratios is the large amplification of seismic waves above about 0.04 Hz at all nonbedrock sites (Figs. 4a, b and 5). In contrast, sites on shallow bedrock other than bedrock reference sites ERW and GNW show little or no amplification except above 0.4–0.5 Hz, where noise levels are starting to be a factor (Fig. 4c). All sites on glacial deposits, both within and outside the deep basins, show strong amplification (5 or more) of both shear- and surface-wave arrivals above 0.1 Hz relative to our bedrock reference sites. The peak amplification occurs at 0.2–0.7 Hz, where amplification values often reach 10 or more. Lack of station coverage does not permit a thorough study of Everett or Tacoma basin effects, but surface-wave amplification reached 10 at the few sites near the Everett basin (Figs. 1 and 4a, b).

Although rock site spectral ratios are clearly distinguished from those at sedimentary sites, the distinction between the deep-basin sites and the nonbasin sedimentary sites is more subtle. All the sites on glacial deposits show little amplification below 0.04 Hz (25-sec period and greater), but between 0.04 Hz and 1 Hz the sedimentary strata substantially amplify seismic waves compared with bedrock. The influence of the deep-basin sediments is seen on the basin spectral ratios (Fig. 4a) as a distinct amplification at and below 0.1 Hz that is missing from the nonbasin sedimentary sites (Fig. 4b). Graphs of the average amplifications for the three classes of sites (Fig. 6) show that between 0.04 and 0.2 Hz the deep-basin sites have about twice the amplification as the other sedimentary sites. These results indicate that the relatively shallow (<2 km) glacial deposits cause most of the observed amplification above 0.2 Hz, and the deep-basin strata increase the amplification in the 0.04- to 0.2-Hz range.

The amplifications we document are in agreement with previous studies of amplification by the Seattle basin (Pratt *et al.*, 2003), which also show peak shear-wave amplifications in excess of 10 at frequencies of 0.3–0.5 Hz (2- to 3.33-sec period). Pratt *et al.* (2003) noted that the largest amplifications were over the east side of the basin. Our results are consistent with this observation (Figs. 2, 5), but we have few permanent stations on the west side of the basin to rigorously test this hypothesis (Fig. 1). Potential explanations for the seismic-wave amplification can be found in Pratt *et al.* (2003) and include resonance, focusing, surface waves, and the low impedance of the basin sediments. The spectral ratios we present here also are consistent with inferences about basin amplification noted elsewhere (e.g., Joyner, 2000). For high frequencies (>1 Hz), in general, it is assumed that the effects of the shallow strata dominate the site response, thus causing sites on glacial deposits outside of the deep basins to show amplification. Both the shallow- and deep-basin strata influence the site response at low frequencies through long-period resonance, focusing, and surface waves (e.g., Joyner, 2000; Pratt *et al.*, 2003).

The large concentration of water-wave observations in the Puget Lowland on top of the basins suggests that the water bodies are especially susceptible to ground motions in the 0.04- to 0.2-Hz frequency range. The maximum ampli-

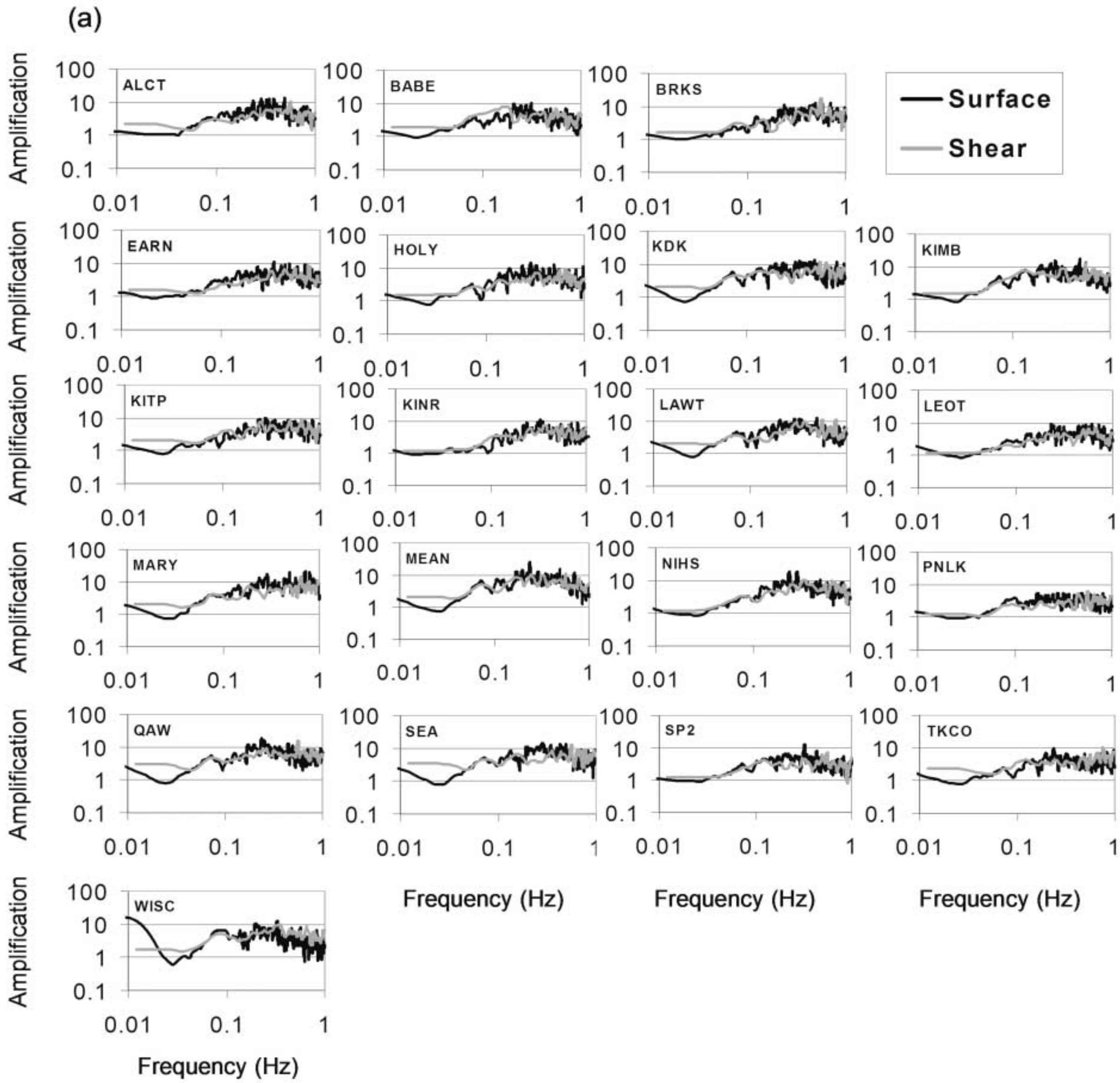

Figure 4. (a) *Deep-basin sediment sites.* Plots of spectral ratios for all stations (shear and surface waves for basin sites) (Seattle and Everett) with respect to the average spectrum of bedrock sites GNW and ERW. The y axis corresponds to amplitude of spectral ratios. (*continued*)

tudes of the Denali arrivals occurred in this frequency range (Fig. 2b). The Puget Lowland may be especially susceptible to seiches during large earthquakes because of the low-frequency seismic-wave amplification by sedimentary basins and other sedimentary structures, plus a concentration of water bodies above the basins.

Seismically Induced Water Waves

Observations from the Denali Earthquake

Long-period seismic waves from the Denali earthquake initiated large waves in water bodies in western Canada (Cassidy and Rogers, 2005) and the United States (Table 1; reports to the PNSN and National Earthquake Information Center for the Pacific Northwest). Water was reported to have surged 1.5 m (5 feet) on the shoreline at Lake Wenatchee in the Cascade Mountains. Broken ice and logs were carried and washed over the shores of several lakes in Washington state. Standing oscillations (seiches) or a series of large waves were set up in other water bodies where floating walkways started moving and boats were slammed against docks.

Some of the most prominent water waves triggered by the Denali earthquake were in Lake Union, in Seattle, Wash-

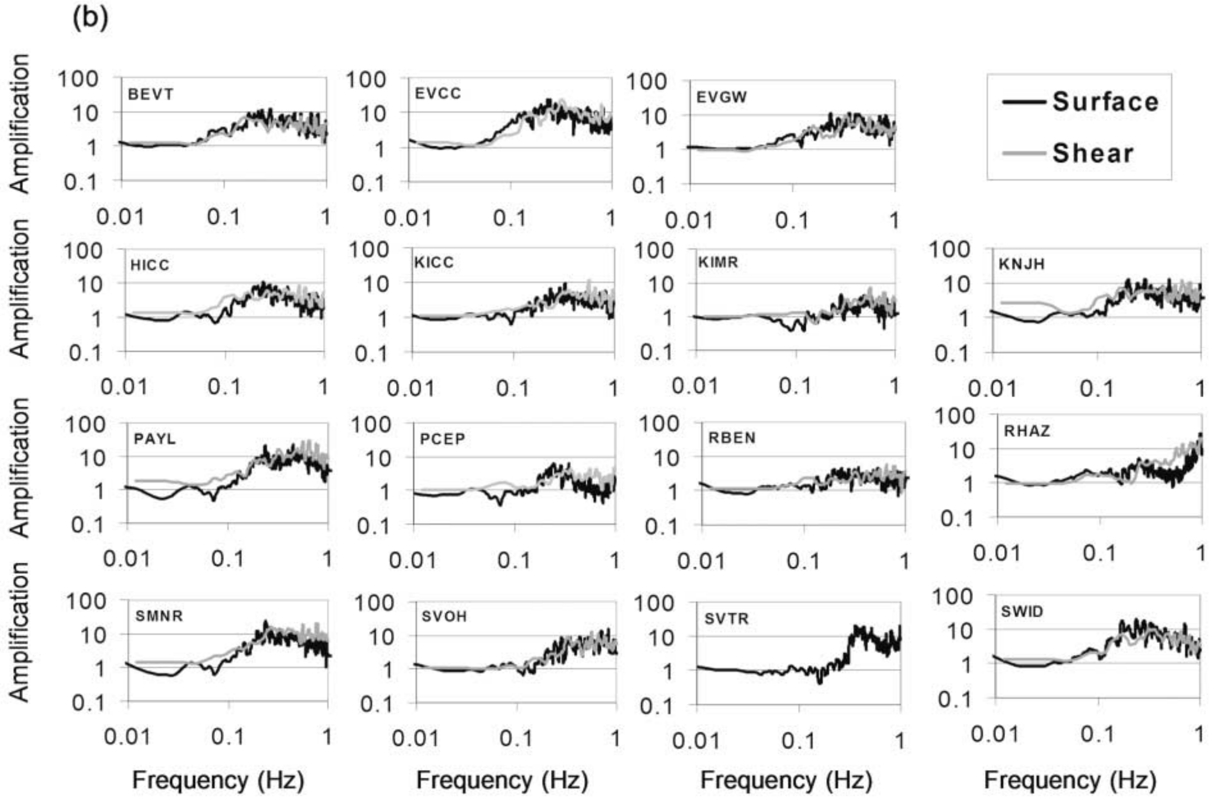

Figure 4. (continued). (b) *Nonbasin glacial sediment sites.* Plots of spectral ratios for all stations (shear and surface waves for nonbasin sites) at sites outside of the Seattle or Everett basins that are located at sedimentary sites. Spectral ratios are computed with respect to the average spectrum of bedrock sites GNW and ERW. The *y* axis corresponds to the amplitude of spectral ratios.

ington, and in an arm of Lake Union named Portage Bay (Table 1) (Barberopoulou *et al.*, 2004). Lake Union is a shallow, Y-shaped lake with the main body having dimensions of about 2 km by 1 km and maximum depths in the different arms varying between 6 and 14 m. More than 20 houseboats on these water bodies sustained minor damage consisting of buckled moorings and broken sewer and water lines. The damage reports were concentrated on the east and west shores of Lake Union and Portage Bay (Barberopoulou *et al.*, 2004). Although this damage pattern might imply water-wave motion in a specific direction, the pattern may also reflect the greater concentration of houseboats along the east and west shores of the lake. Water waves were reported on Lake Washington, which also overlies the Seattle basin, but because of the lack of houseboats on the shores of Lake Washington there were fewer observations of damage there than around Lake Union.

Sloshing action was also reported in swimming pools and ponds around Seattle (Table 1). Residential swimming pools overflowed or showed large water oscillations in the north–south direction, which is approximately the direction from which the seismic waves arrived and may indicate the effect of Rayleigh waves (Table 1). Many of the pools with reported oscillations in Seattle are public facilities or private clubs with pool lengths of 17–25 m. A typical residential swimming pool where sloshing was observed was 11 m (36 feet) long and 5.5 m (18 feet) wide with an average depth of 2 m.

The distribution of these water-wave reports is obviously biased by population density and demographic factors, but the density of reports shows a close correspondence with the largest ground motions recorded on PNSN seismographs. In particular, from the 49 reports collected for Washington state 41 fall within the latitude and longitude limits of Figure 1. All the observations in the Seattle basin (thirty in total) were clustered over the deepest, central part of the basin despite large areas of dense population outside of the boundary of the Seattle basin near a variety of water bodies for which reports are lacking. Based on this correlation we believe that basin amplification was an important factor contributing to damaging water waves over the Seattle basin (Fig. 6). McGarr and Vorhis (1968) suggested that seiches from distant earthquakes most commonly occur in areas where the seismic waves with periods of 5–15 sec are amplified by local geologic structures such as sedimentary basins. As noted earlier, our comparison of spectral ratios in-

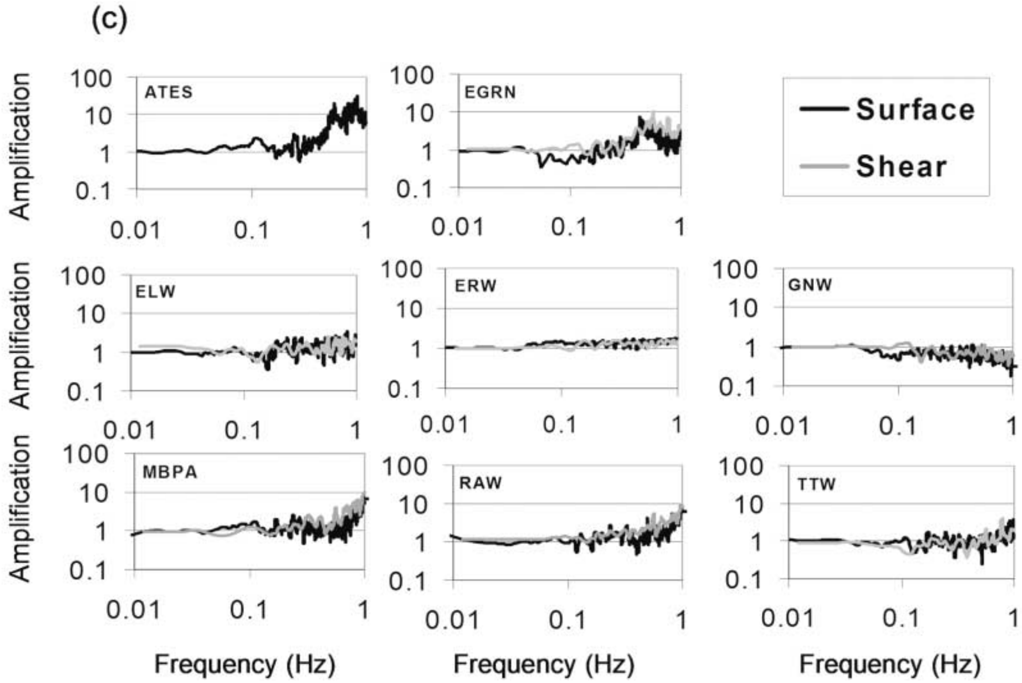

Figure 4. (continued). (c) *Rock and nearly rock sites.* Plots of spectral ratios corresponding to stations situated at bedrock or nearly bedrock sites. Missing shear-wave spectral ratios correspond to stations with very high signal-to-noise ratio or malfunctioning instrument with no signal recorded. ERW and GNW are the reference sites used.

side and outside the basins (Fig. 6) suggest that seismic waves in the frequency range of 0.04 to 0.2 Hz caused the most prominent water waves to be concentrated over the deep sedimantary basins.

Large water waves from past regional or distant earthquakes have been reported in local newspapers in Seattle (Table 2), and Lake Union, in particular, has experienced many seismically induced water waves in the past. Newspaper accounts show that large-amplitude water waves occurred in various water bodies across Washington state during the 1891 Port Townsend earthquake (*The Oregonian*, 29 November 1891), the 1899 Yakutat Bay Alaska earthquake (Dow, 1964), the 1906 San Francisco earthquake (*Seattle Post-Intelligencer*, 19 and 25 April 1906), the *M* 7.1 1949 Olympia earthquake (*The Seattle Times*, 14 April 1949), the M_w 9.2 1964 Alaska earthquake (*The Seattle Times*, 29 March 1964), and the *M* 6.5 1965 Seattle-Tacoma earthquake (*The Seattle Times*, 19 and 30 April 1965). Damage during the 1964 Alaska earthquake was, as during the Denali earthquake, concentrated around Lake Union and Portage Bay in Seattle.

With one exception, we have no water-level recordings of seismically induced water waves in Washington state from the Denali earthquake, or from any previous earthquakes, that are suitable to analyze wave motions in detail. Water levels are generally sampled only once every few minutes, or less frequently, to measure tide or reservoir levels. The gauges are often damped to filter out the short-period waves caused by wind and boats. Although long-period seiches in bodies of water with fundamental periods of hours are adequately sampled, short-period seiches induced by seismic waves are not. Therefore, our analysis is almost entirely limited to testing whether modeling results match the approximate wave heights reported by eyewitness accounts.

National Oceanographic and Atmospheric Administration (NOAA) tide gauge stations in Puget Sound provide some scant evidence of water waves caused by the Denali earthquake. The highest data rate recorded by these stations is 6-min sample intervals and each water-level datum is averaged over 3 min, centered on the reporting time. As expected, the averaged water-level data do not show a clear record of seismically induced seiches. However, NOAA also computes root-mean-square (rms) wave heights that are sampled every 1 sec but averaged in the same way as the water level. Several Alaska tide gauges show rms peaks resulting from seismic waves from the Denali earthquake, and in Washington, a tide gauge in Tacoma shows a particularly prominent rms peak at the expected time (Fig. 7a, c).

A theoretical rms was computed to test whether the Tacoma rms wave-height recording was indeed a record of a seiche due to ground shaking from long-period seismic waves. We computed the rms we would expect at the Tacoma tide gauge from the Denali earthquake assuming that the seiche amplitude time-history is a scaled version of the accelerogram recorded at a station near Tacoma (seismic

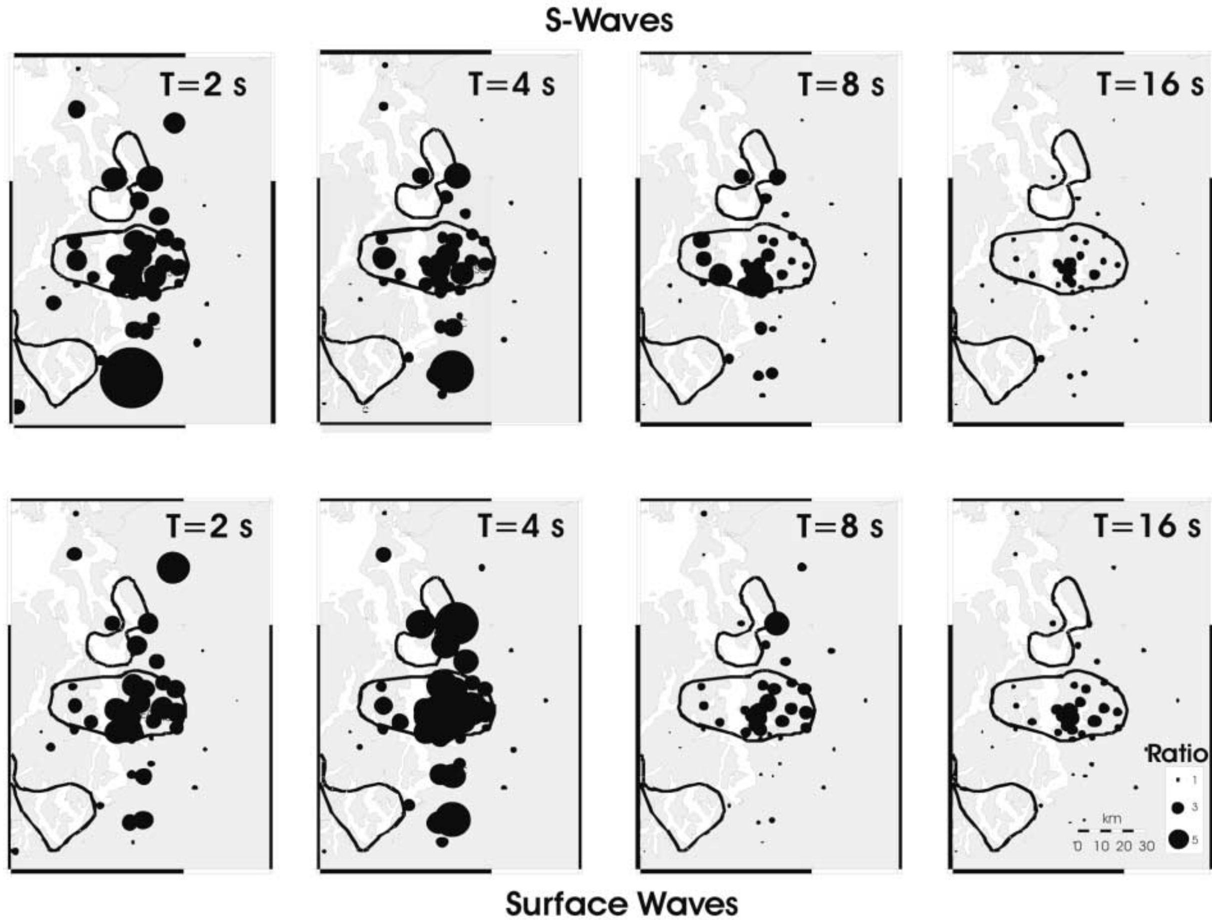

Figure 5. Dot maps showing amplification of horizontal ground motion at strong motion sites relative to the motion on bedrock for wave periods of 2, 4, 8, and 16 sec (0.5, 0.25, 0.125, and 0.0625 Hz). The four maps in the top row show amplification of *S* waves. The four maps at the bottom show surface-wave amplification. The computations are done for horizontal "transverse" motion (motion perpendicular to a line between the epicenter and the Puget lowland). Dot size is proportional to the spectral ratio (SiteSpectrum/RockSpectrum) at each period. The rock spectrum is the average of two rock sites (ERW, GNW). Stations enclosed by the heavy contours are defined as basin sites. Area is the same as Figure 1.

trace at the top of Figure 7). We computed the resulting rms wave height versus time using the same algorithm as is used at the NOAA tide gauges. If we constrain the maximum values of the observed and computed rms amplitudes to be equal, we obtain an excellent match for the duration of the observed and computed rms time histories (Fig. 7a). From the computed rms amplitude, we conclude that the maximum amplitude of the waves at the Tacoma tide gauge was about 26 cm (0-peak) which is of the same order as amplitudes anecdotally reported from other bodies of water in the Puget Lowland (Table 1).

The rms wave-height peaks at other tide gauges in the Puget Sound region were not nearly as prominent as at Tacoma. We believe this is because the Tacoma gauge is located in a ship channel about 140 m wide that is bounded by vertical walls. It is therefore likely that any seismically generated waves observed at the gauge would be locally generated within the channel, rather than waves that had propagated across Tacoma port/Commencement Bay. The amplitudes of such waves within the channel must vary greatly with location, especially relative to distance from the sidewalls (e.g., cross-channel slosh modes). Hence it would be difficult to extrapolate the interpretation of seiche measurements at the gauge to other locations in the Port of Tacoma (Commencement Bay). The tide gauge station in Seattle would be the obvious choice to analyze in a similar fashion, but the instrument is located at the Ferry terminal on a busy waterfront and the data are therefore contaminated by high-frequency noise due to waves from ship traffic (Fig. 7c).

With the exception of the Tacoma tide-gauge record, we can only compare our theoretical results with observers' reports. Most observers estimated that water-wave action in the Seattle area lasted 1 to 5 minutes, which corresponds well with the approximately 300-sec duration of the largest

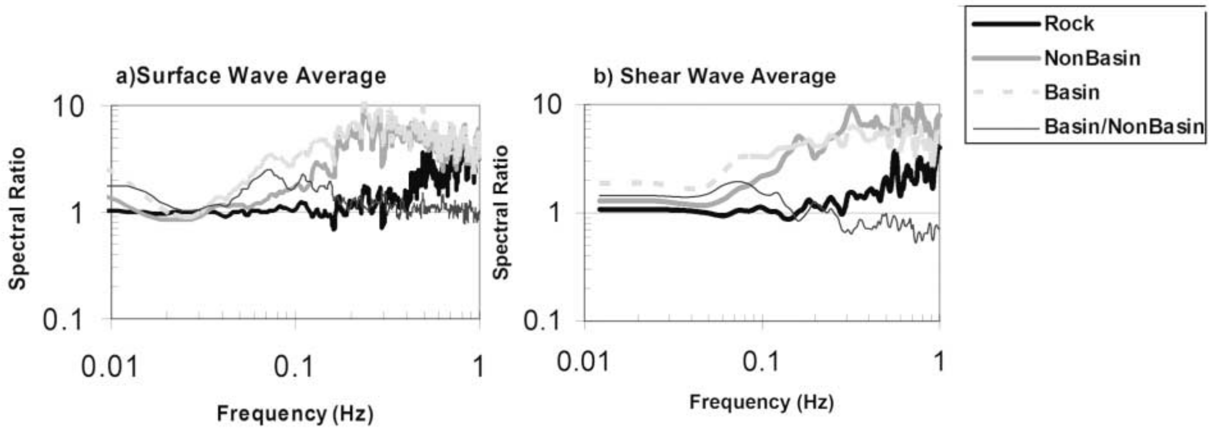

Figure 6. Average of spectral ratios (see Fig. 4) of basin, nonbasin, and rock sites with respect to two reference stations (GNW, ERW). (a) Surface waves. (b) Shear waves. Nonbasin sites show significant amplification because they also overlie sediments, although not as thick as the basin sediments. The thin black line represents the ratio of basin to nonbasin spectral ratios. The difference between the basin and nonbasin curves is most pronounced for surface waves at frequencies of 0.04–0.2 Hz.

surface waves recorded by the PNSN seismographs (Table 1). Some observers reported wave periods of 5–20 sec (Table 1), in general agreement with the 10–12-sec period of the largest surface waves. A few reports contained a rough estimate of the number of cycles (8–10), but these estimates must reflect just the largest wave motions because the observed duration of motion was reported to be considerably longer than 80–100 sec. Many observers reported water moving back and forth horizontally with little vertical motion. Reported vertical amplitudes, observed primarily at swimming pools where the waves overtopped the sides of the pools, were typically 30 cm. On large bodies of water people reported horizontal runup of 0.6–3 m on the shore, with most observers reporting about 1 m.

Water Wave Modeling

Lamb (1932) developed the shallow-water approximation for standing water waves in basins of rectangular cross section (uniform depth) and variable depth. The earliest studies of earthquake-induced seiches may be attributed to Kvale (1953) and Proudman (1953). A basic mechanism for the generation of seismically induced water waves by the horizontal motion of the sides of the water body has been presented by McGarr (1965). McGarr and Vorhis (1968), and Ruscher (1999) have also studied seismically induced seiches. However, the fluid mechanics literature contains analyses of the sloshing of fluids in rectangular tanks, in particular, as applied to tanks in ships (e.g., Waterhouse, 1994; Faltinsen *et al.*, 2000; Hill, 2003). The application of these latter methods to lakes of arbitrary shapes with variable sides has not been tested. Wind- and tsunami-induced seiches in lakes and open bodies of water have been better studied, with recent work carried out by Ichinose *et al.* (2000), Zacharias (2000), and Rueda and Schladow (2002).

In the 36 years since the McGarr and Vorhis study, seiches induced by seismic events have received little examination. Unlike previous earthquakes known for generating seiches (e.g., the 1964 Alaska earthquake), ground motions during the Denali earthquake were well recorded on a variety of seismometers worldwide. The Denali earthquake therefore provides us with an opportunity to examine ground motions that initiate seiches in water bodies at large distances.

Barberopoulou *et al.* (2004) did some analysis for the surface oscillations setup in water bodies during the Denali earthquake. It was found that a residential swimming pool of 10 m width and 2 m depth has a fundamental period of oscillation of 4.5 sec (0.2 Hz), a period that was strongly excited by seismic waves from the Denali earthquake (Fig. 2). This estimate is in agreement with the observations of sloshing in swimming pools during the earthquake (Table 1). Therefore resonance in the fundamental mode is a reasonable explanation for the surface oscillations induced in swimming pools during the Denali earthquake. Figure 8 shows that the Denali earthquake, with dominant wave periods of 10 to 30 sec, could set shallow water bodies with widths of 20 to 300 m into fundamental mode resonance. The 10- to 30-sec periods (0.1–0.033 Hz) are also the periods that the deep Seattle basin amplifies relative to the glacial deposits, making these periods the most likely to produce fundamental mode seiches.

The predicted fundamental periods of sections of Lake Union (approximately 200 sec; Barberopoulou *et al.*, 2004) are longer than the dominant periods of the seismic surface waves, and the water-wave periods described in the eyewitness reports. Seismic amplitudes from the Denali earthquake at 100 sec (0.01 Hz) are relatively low, far smaller than the amplitudes at 10-sec periods (0.1 Hz) that dominate the surface-wave signal (Fig. 2). Furthermore, long-period seismic

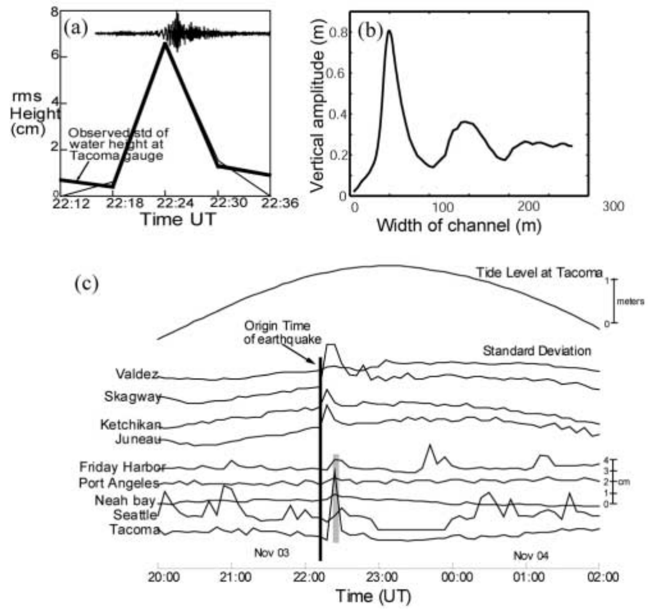

Figure 7. (a) Heavy line shows the recorded rms deviation of wave height recorded at the NOAA Tacoma, Washington, tide gauge on 3 November 2002. Root mean square (rms) is sampled every 6 min, and each point is computed for a 3-min window centered at the sample time. The rms is computed from wave-height deviations that are sampled every second. The light line is the computed rms deviation assuming the water waves are a scaled version of an actual seismogram of the Denali earthquake recorded at a station near Tacoma (illustrated at the top of the figure using the same time scale). To scale the wave heights so that the peaks of both rms curves match at 6.6 cm requires that the maximum 0-to-peak water wave amplitude at the gauge was about 26 cm. (b) Computed response of a channel 8 meters deep to surface waves (east component recorded at station WISC). The graph shows the maximum vertical amplitude of wave motion as a function of channel width using a reflection coefficient of 0.9 at the walls of the channel. (c) rms heights recorded in Alaska and Washington states. The names of the tide gauge locations appear on the left. The top four traces are from locations in Alaska whereas the bottom five correspond to locations in Washington state. The origin time of the earthquake in local time in Alaska is shown by the solid vertical line.

waves (>10 sec) undergo relatively modest amplification within the Seattle basin compared with waves of shorter period (Figs. 4 and 6). Such long water-wave periods also conflict with observers' reports, which describe a series of waves 5–20 sec apart.

The mismatch between the fundamental period of sections of Lake Union and the periods of observed water waves can be explained by higher-order modes of resonance excited by the seismic forcing. Surface waves from the Denali earthquake provided 10–30 cycles of motion over a 100- to 300-sec period (Fig. 2). This is a sufficiently long duration of forcing to excite higher modes of resonance.

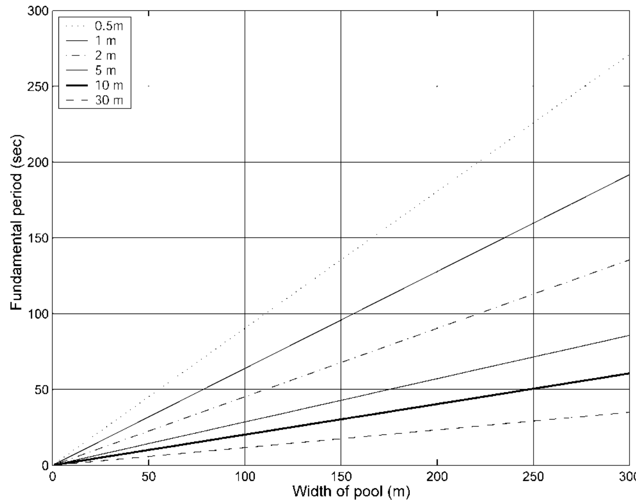

Figure 8. Lines showing the change in fundamental period as a function of width for a swimming pool with the range of depths shown at the inset. Merian's formula has been used for the calculation of the period (Lamb, 1932; Proudman 1953).

We model the response of swimming pools and portions of Lake Union using a simple model of a water body ("canal") of rectangular cross section and infinite length (Lamb, 1932; Russell and Macmillan, 1952; Proudman, 1953; McGarr, 1965; Wilson, 1972). Following Lamb (1932) and Proudman (1953) we assume a water body with vertical boundaries at distances $x = 0$ and L. We constrain the motion in the x-z plane (one-dimensional flow) and simplify the geometry by assuming a flat, horizontal bottom. In this model, horizontal motion of the sides of the water body generate water waves that constructively interfere with waves generated at the opposite wall.

In the rectangular model we assume that energy is fed into the water body through the horizontal movement of its boundaries (McGarr, 1965). Because we consider long-period motion (seismic surface waves have wavelength of several kilometers) we assume the forced walls of the water body to be moving in the same direction at the same time (i.e., the water body is much smaller than a half-wavelength). Then it can be shown that the water elevation η at any time t and point x is given by equation (1) (McGarr, 1965):

$$\eta(x,t) = \frac{4h}{\pi c} \sum_{n=0}^{\infty} \frac{\cos[(2n+1)\pi x L^{-1}]}{2n+1} \int_0^t F(\tau) e^{-k(t-\tau)/2} \sin\left[\frac{(2n+1)\pi c(t-\tau)}{L}\right] d\tau, \quad (1)$$

where F is the forcing function (horizontal ground acceleration), k a damping constant, h the depth of the water body (constant in our case), $c = \sqrt{gh}$ the wave velocity, and L the distance between the boundaries of the water body.

In this model the forcing is applied at the boundaries ($x = 0, L$) and the response of the water surface is "measured" at a selected position x between the walls. As a forcing function, we used a ground motion recording from station WISC near Lake Union (Fig. 9a). For computations we used a modified version of equation 1 (H. Mofjeld, personal comm., 2004) with the forcing input being ground velocity rather than acceleration. The elevation of the water at any point x and time t is given by the superposition of reflected and incident waves off the boundary walls.

The rectangular model (Fig. 9) gives reasonable estimates for the large swimming pools, with computed wave heights in excess of 0.3 m being consistent with observations of water sloshing over the sides of the pools. We set the width of the large pool (22.1 m) to match the period of the pool's fundamental mode with the period of the largest seismic waves, in an attempt to find the maximum expected water-wave amplitudes. Such dimensions for a swimming pool are within the range of 17–25 m that are standard for pools in schools, country, and sport clubs where many of the observations of sloshing originated. For small pools the model predicts only 4-cm wave heights, which are large enough to be noticeable but too small to cause sloshing over the sides of the pools (Fig. 9). The simple model indicates that a cross section of Lake Union (width, 800 m) would produce water waves with amplitudes of up to 20 cm. We know that amplitudes were large enough to be noticeable, with the collection of reports suggesting water-wave heights of at least 30 cm along the shores of the lakes. Considering the uncertainty and incompleteness in the observations, the model agrees fairly well with the vertical motions of the water observed in the swimming pools but may slightly underestimate those in Lake Union.

To demonstrate the effect the Seattle basin has on water bodies we have computed water levels using the accelerogram recorded by station WISC (Seattle basin) and station GNW (bedrock; Figs. 9 and 10). The seismic waves recorded at GNW would not produce large surface oscillations in any of the water bodies we considered. The predicted water-surface oscillations for location GNW do not exceed 2 cm. Water bodies located on the basins would produce water waves about 10 times as large (Figs. 9 and 10).

Most estimates of the vertical amplitude of the water level during the Denali earthquake are derived from observations of swimming pools. We do not have many estimates around the lakes and only a few estimates refer to vertical motion at Lake Union. Most observations from lakes in the Puget Lowland refer to horizontal displacements or runup distance on the shore. These runup distances are often large (1–5 m) but depending on the sloping beach the vertical

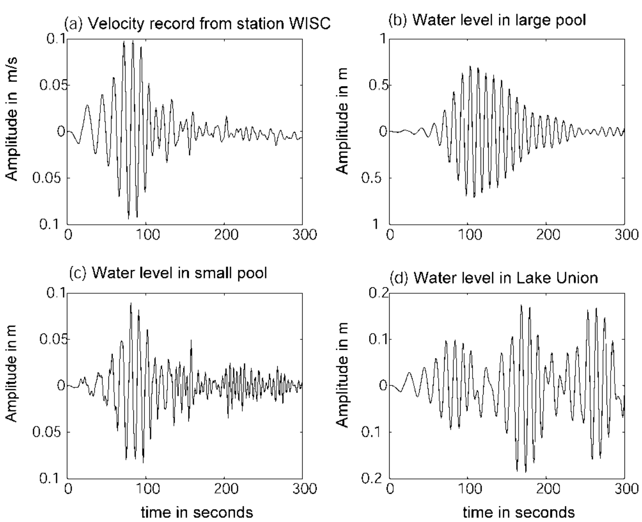

Figure 9. Expected wave heights for three rectangular water bodies subjected to the horizontal ground motion recorded at Seattle basin station WISC during the Denali earthquake. (a) Velocity record section of east component at WISC station is used as input to our model. (b) Computed wave height at the edge of a large pool whose dimensions (width, 22.1 m; depth, 2 m) are chosen to provide a fundamental period of 10 sec. (c) Computed wave height in a small pool of width 10 m and depth 2 m. Note scale factor of 10^{-3}. (d) Computed wave height in Lake Union (width, 800 m; depth, 8 m). In all cases a reflection coefficient of 0.9 is assumed for waves that bounce back and forth between the walls of the basin.

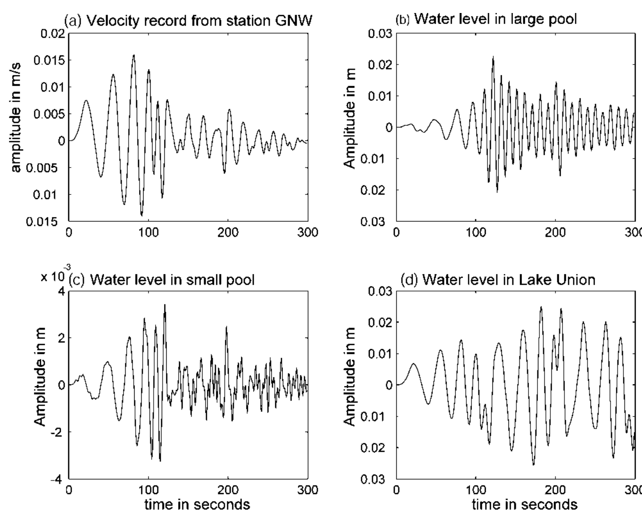

Figure 10. Expected wave heights for three rectangular water bodies subjected to the horizontal ground motion recorded at reference station GNW during the Denali earthquake. (a) Velocity record section of east component at GNW station is used as input to our model. (b) Computed wave height at the edge of a large pool whose dimensions (width, 22.1 m; depth, 2 m) are chosen to provide a fundamental period of 10 sec. (c) Computed wave height in a small pool of width 10 m and depth 2 m. (d) Computed wave height in Lake Union (width, 800 m; depth, 8 m). In all cases a reflection coefficient of 0.9 is assumed for waves that bounce back and forth between the walls of the basin.

heights they correspond to can be much smaller (i.e., 20–30 cm). The lack of water-level measurements makes it difficult to conclude how well our simple model approximates the true wave motions.

Despite these uncertainties we can still use the rectangular model to estimate wave heights in Lake Union during other types of earthquakes. Since the accelerometers of the PNSN were installed, the only major local earthquake recorded was the 2001 M_L 6.8 Nisqually earthquake. We have used the recording of the Nisqually earthquake from seismic station WISC in the Seattle basin as input to the model (Fig. 11). Under Nisqually earthquake forcing we see water-wave amplitudes that are comparable to those calculated for the Denali event (Fig. 11) although their frequency is much higher than the water waves produced by the low-frequency Denali surface waves. We note that no unusual water waves were reported during the Nisqually earthquake.

The absence of observed seiches and the results of the model appear to agree that water waves were not considered unusual during the Nisqually earthquake. The frequency content of the Nisqually earthquake signal was much higher than that of the Denali. This would not be surprising given that the Nisqually earthquake is a local deep (52 km) event generating relatively small surface waves compared with near-surface events. The signal from the distant Denali earthquake in Washington included long periods and duration and generated unusual water motion (easily noticeable) unlike that produced by ship traffic or winds. In contrast the higher-frequency wave motion during the Nisqually earthquake probably was either confused with other generating sources (i.e., ship traffic) by observers who were also distracted by the strong shaking and damage caused by the earthquake, or the water activity was not surprising enough for observers to report. A few observations of water waves were made during the 1949 and 1965 earthquakes (Table 2). These earthquakes were similar to the Nisqually earthquake in location, magnitude, and depth (54 and 63 km).

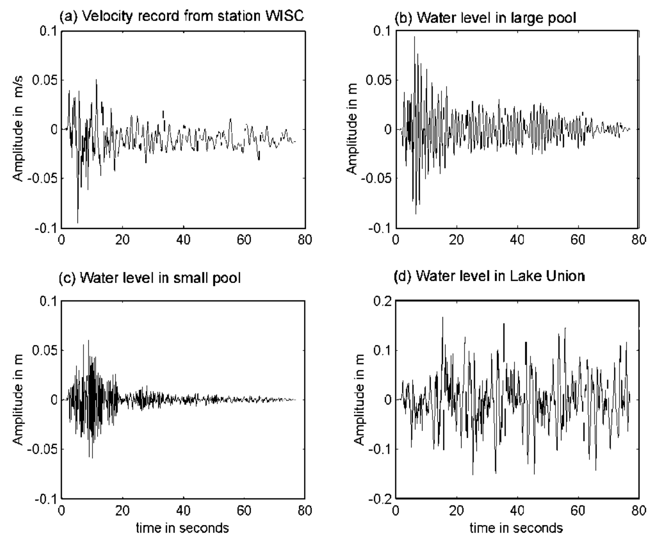

Figure 11. Expected wave heights for three rectangular water bodies under Nisqually earthquake forcing. (a) Velocity record section at WISC station is used as input to our model. (b) Computed wave height at the edge of a large pool whose dimensions (width, 22.1 m; depth, 2 m) are chosen to provide a fundamental period of 10 sec. (c) Computed wave height in a small pool with width, 10 m, depth, 2 m. (d) Computed wave height in Lake Union (width, 800 m; depth, 8 m). In all cases a reflection coefficient of 0.9 is assumed for waves that bounce back and forth between the walls of the basin.

Discussion and Conclusions

We used the spectral-ratio technique to document the amplification of long-period seismic waves by the Seattle basin, shallow glacial sediments, and bedrock sites. We find large amplification at frequencies of 0.2–1 Hz, which is in agreement with previous studies (Pratt *et al.*, 2003), but we also see amplification at longer periods. Most of the amplification we observe is caused by shallow deposits, whereas the deep basin strata further amplify waves at frequencies of 0.04–0.2 Hz (5 to 25-sec period). Spectral ratios confirm that there is amplification at other locations outside of the Seattle basin where sedimentary deposits overlay the bedrock.

In an effort to explain the generation of water waves in Lake Union, we have used a simple model of a rectangular basin to compute water-wave heights due to prolonged seismic forcing of water bodies. The forcing functions we used were seismic recordings of the distant, Denali earthquake and recordings made in Seattle during the deep Nisqually earthquake of 2001. This model predicts amplitudes in Lake Union of ~20 cm during the Denali earthquake and comparable water-wave amplitudes during the Nisqually earthquake. The absence of reported water activity during the Nisqually may be due to the higher frequency content and shorter duration of the Nisqually signal.

Despite demographics, there is a remarkable correlation between the distribution of water-wave reports during the Denali earthquake and the largest seismic wave amplification in the Puget Lowland. The documented long-period amplification by the sedimentary basins underlying the Puget Lowland, and the results of our simple model suggest that the water waves observed in Lake Union were caused by prolonged seismic forcing caused by the amplified waves in the Seattle basin.

Although the results do provide suggestions for what caused the unusual water motion they also highlight the need for further investigation using more realistic models and examination of other types of earthquakes. In particular, a complete investigation would have to include the full geometry of the lake. The latter is important since variable bathymetry and shoreline (among other things) may be responsible for enhanced wave heights in selected locations through focusing. Since the 1964 Alaska earthquake, a comprehensive water-level-recording network, including tide gauges operating at the time of that earthquake, has largely been removed, resulting in much less water-level data to work with. Estimates could be significantly improved using instrumentation to record water levels at high-frequency rates in key locations because this would provide data for model testing.

Acknowledgments

We thank the Advanced National Seismic System (ANSS) for partial financial support of the strong-motion network and Ruth Ludwin for the information about the 1899 Alaska earthquake. We especially thank Harold Mofjeld for his help with the tide gauge instruments and the computer modeling. We thank Tom Brocher, Art McGarr, Paul Bodin, and the two anonymous reviewers. Their suggestions significantly improved the final version of this manuscript.

References

Barberopoulou, A., A. Qamar, T. L. Pratt, K. C. Creager, and W. P. Steele (2004). Local amplification of seismic waves from the Denali Earthquake and damaging seiches in Lake Union, Seattle, Washington, *Geophys. Res. Lett.* **31,** L03607, doi 10.1029/2003GL018569.

Booth, D. B. (1994). Glaciofluvial infilling and scour of the Puget Lowland, Washington, during ice-sheet glaciation, *Geology* **22,** 695–698.

Brocher, T. M., R. J. Blakely, and R. E. Wells (2004). Interpretation of the Seattle Uplift, Washington as a passive roof duplex, *Bull. Seism. Soc. Am.* **94,** 1379–1401.

Brocher, T. M., T. Parsons, R. J. Blakely, N. I. Christensen, M. A. Fisher, and R. E. Wells, and SHIPS Working Group (2001). Upper crustal structure in Puget Lowland, Washington: results from the 1998 Seismic Hazards Investigation in Puget Sound, *J. Geophys. Res.* **106,** 13,541–13,564.

Cassidy, J. F., and G. C. Rogers (2005). The M_w 7.9 Alaska earthquake of 3 November 2002: felt reports and unusual effects across western Canada, *Bull. Seism. Soc. Am.* **94,** no. 6B, S53–S58.

Crosson, R. L., and T. L. Owens (1987). Slab geometry of the Cascadia subduction zone beneath Washington from earthquake hypocenters and teleseismic converted waves, *Geophys. Res. Lett.* **14,** 824–827.

Donn, W. L. (1964). Alaskan earthquake of 27 March 1964: remote seiche simulation, *Science* **145,** 261–262.

Dow, E. (1964). *Passes to the North: History of Wenatchee Mountains*, Wenatchee Bindery and Printing Company, Wenatchee, Washington.

Eberhart-Phillips, D., P. J. Haeussler, J. T. Freymueller, A. D. Frankel, C. M. Rubin, P. Craw, N. A. Ratchkovski, G. Anderson, G. A. Carver, A. J. Crone, T. E. Dawson, H. Fletcher, R. Hansen, E. L. Harp, R. A. Harris, D. P. Hill, S. Hreinsdóttir, R. W. Jibson, L. M. Jones, R. Kayen, D. K. Keefer, C. F. Larsen, S. C. Moran, S. F. Personius, G. Plafker, B. Sherrod, K. Sieh, N. Sitar, and W. K. Wallace (2003). The 2002 Denali fault earthquake, Alaska: a large magnitude, slip-partitioned event, *Science* **300,** 1113–1118.

Faltinsen, O. M., O. F. Rognebakke, I. A. Lukovsky, and A. N. Timokha (2000). Multidimensional modal analysis of nonlinear sloshing in a rectangular tank with finite water depth, *J. Fluid Mech.* **407,** 201–234.

Frankel, A., and W. Stephenson (2000). Three-dimensional simulations of ground motions in the Seattle region for earthquakes on the Seattle fault zone, *Bull. Seism. Soc. Am.* **90,** 1251–1267.

Frankel, A. D., D. L. Carver, and R. A. Williams (2002). Nonlinear and linear site response and basin effects in Seattle for the M6.8 Nisqually, Washington, earthquake, *Bull. Seism. Soc. Am.* **92,** 2090–2109.

Galster, R. W., and W. T. Laprade (1991). Geology of Seattle, Washington, United States of America, *Bull. Assoc. Eng. Geol.* **28,** 235–302.

Hartzell, S. (1992). Site response estimation from earthquake data, *Bull. Seism. Soc. Am.* **82,** 2308–2327.

Hill, D. F. (2003). Transient and steady-state amplitudes of forced waves in rectangular basins, *Phys. Fluids* **15,** 1576–1587.

Ichinose, G. A, J. G. Anderson, K. Satake, R. A. Schweickert, and M. M. Lahren (2000). The potential hazard from tsunami and seiche waves generated by large earthquakes within Lake Tahoe, California–Nevada, *Geophys. Res. Lett.* **27,** 1203–1206.

Johnson, S. Y., R. J. Blakely, W. J. Stephenson, S. V. Dadisman, and M. A. Fisher (2004). Active shortening of the Cascadia forearc and implications for seismic hazards of the Puget Lowland, *Tectonics* **23,** TC1011, doi 10.1029/2003TC001507.

Johnson, S. Y., C. J. Potter, and J. M. Armentrout (1994). Origin and evolution of the Seattle fault and Seattle basin, Washington, *Geology* **22,** 71–74.

Johnson, S. Y., C. J. Potter, J. M. Armentrout, J. J. Miller, C. Finn, and C. S. Weaver (1996). The southern Whidbey Island fault: an active structure in the Puget Lowland, Washington, *Geol. Soc. Am. Bull.* **108,** 334–354.

Jones, M. A. (1996). Thickness of unconsolidated deposits in the Puget Sound Lowland, Washington and British Columbia, *U.S. Geol. Surv. Water Resour. Invest. Rept. 94-4133*.

Joyner, W. B. (2000). Strong motion from surface waves in deep sedimentary basins, *Bull. Seism. Soc. Am.* **90,** S95–S112.

Koketsu, K., K. Hatayama, T. Furumura, Y. Ikegami, and S. Akiyama (2005). Damaging long-period ground motions from the 2003 M_w 8.3 Tokachi-oki, Japan, Earthquake, *Seism. Res. Lett.* **76,** 67–73.

Korgen, B. J. (1995). Seiches, *Am. Scientist* **83,** 330–341.

Kvale, A. (1953). Seismic seiches in Norway and England during the Assam earthquake of August 15, 1950, *Bull. Seism. Soc. Am.* **45,** 93–113.

Lamb, H. (1932). *Hydrodynamics*, Dover, New York.

McGarr, A. (1965). Excitation of seiches in channels by seismic waves, *J. Geophys. Res.* **70,** 847–854.

McGarr, A., and R. C. Vorhis (1968). Seismic Seiches from the March 1964 Alaska Earthquake, *U.S. Geol. Surv. Profess. Pap. 544E*, E1–E43.

Pratt, T. L., and T. M. Brocher (2006). Site response and attenuation in the Puget Lowland, Washington State, *Bull. Seism. Soc. Am.* **96,** no. 2, 536–552

Pratt, T. L., T. M. Brocher, C. S. Weaver, K. C. Miller, A. M. Trehu, K. C. Creager, and R. S. Crosson (2003). Amplification of seismic waves by the Seattle basin, Washington State, *Bull. Seism. Soc. Am.* **93,** 533–545.

Pratt, T. L., S. Johnson, C. Potter, W. Stephenson, and C. Finn (1997). Seismic reflection images beneath Puget Sound, western Washington state: the Puget Lowland thrust sheet hypothesis, *J. Geophys. Res.* **102,** 27,469–27,489.

Proudman, J. (1953). *Dynamical Oceanography*, Methuen, London.

Rueda, F. J., and S. G. Schladow (2002). Surface seiches in lakes of complex geometry, *Limnol. Oceanogr.* **47,** 906–910.

Ruscher, C. R. (1999). The sloshing of trapezoidal reservoirs, *Ph.D Thesis*, University of Southern California, Los Angeles, California.

Russell, R. C. H, and D. H. Macmillan (1952). *Waves and Tides*, Hutchinson's Scientific and Technical Publications, New York.

Snelson, C. M., K. C. Miller, T. M. Brocher, T. L. Pratt, A. M. Tréhu, and C. S. Weaver (2000). Results of the 1999 Dry SHIPS (Seismic Hazard Investigations of Puget Sound) Seismic Experiment in western Washington, *Eos Trans. AGU* **81,** F871.

ten Brink, U. S., P. C. Molzer, M. A. Fisher, R. J. Blakely, R. C. Bucknam, T. Parsons, R. S. Crosson, and K. C. Creager (2000). Subsurface geometry and evolution of the Seattle fault zone and the Seattle basin, Washington, *Bull. Seism. Soc. Am.* **92,** 1737–1753.

Thorson, R.M. (1980). Ice-sheet glaciation of the Puget Lowland, Washington, during the Vashon Stade (Late Pleistocene), *Quat. Res.* **13,** 303–321.

Van Wagoner, T. M., R. S. Crosson, K. C. Creager, G. Medema, L. Preston, N. P. Symons, and T. M. Brocher (2002). Crustal structure and relocated earthquakes in the Puget Lowland, Washington from high resolution seismic tomography, *J. Geophys. Res.* **107,** no. B12, 22-1–22-23.

Waterhouse, D. D. (1994). Resonant sloshing near a critical depth, *J. Fluid Mech.* **281,** 313–318.
Wilson, B. W. (1972). *Seiches*, in *Advances in Hydrosciences*, V.-T. Chow (Editor), Academic Press, New York.
Zacharias, I. (2000). Verification of seiching processes in a large and deep lake (Trichonis, Greece), *Mediterr. Mar. Sci.* **1,** 79–89.

Department of Earth and Space Sciences
University of Washington
Seattle, Washington 98195
(A.B., A.Q., W.P.S.)

Anthony Qamar died in an automobile accident on 4 October 2005.

U.S. Geological Survey, School of Oceanography
University of Washington
Seattle, Washington 98195
(T.L.P.)

Manuscript received 2 May 2005.